

MONTE CARLO SIMULATIONS OF ROD-LIKE GAY BERNE MESOGENS WITH TRANSVERSE DIPOLES

ROBERTO BERARDI, SILVIA ORLANDI, and CLAUDIO ZANNONI*

*Departimento di Chimica Fisica ed Inorganica dell' Università, Viale Risorgimento 4
40136 Bologna, Italy*

**E-mail: vz3bod7a@sirio.cineca.it*

Received 30 July 1998

We report the results of a Monte Carlo investigation of a system of rod-like particles interacting via the Gay-Berne potential with an embedded transverse dipole. We describe the effect that the dipole has on the molecular organization.

Keywords: Computer Simulations; Liquid Crystals; Dipolar Systems.

1. Introduction

The study of the relationship between a certain molecular structure and the types of liquid crystalline mesophases¹ that can be obtained at given thermodynamic conditions as well as the properties of the mesophases, if any, that are actually formed, is a subject of great current interest. On one hand, there is the fundamental issue of identifying the minimum set of molecular features required for a certain collective organization to be produced. On the other, given the technological importance of liquid crystals in the display device industry, there is the more immediately practical issue of designing new liquid crystals with specific properties and of optimizing the existing ones.

In the effort of coming to grips with this difficult problem, molecular scale models, such as those based on the Gay-Berne (GB) potential² have proved to be very useful. The GB potential has a repulsive and attractive contribution with a 12-6 inverse distance dependence form:

$$U_{GB} = 4\epsilon_0\epsilon(\hat{\mathbf{u}}_i, \hat{\mathbf{u}}_j, \hat{\mathbf{r}}) \times \left[\left\{ r - \sigma(\hat{\mathbf{u}}_i, \hat{\mathbf{u}}_j, \hat{\mathbf{r}}) + \sigma_s \right\}^{12} - \left\{ r - \sigma(\hat{\mathbf{u}}_i, \hat{\mathbf{u}}_j, \hat{\mathbf{r}}) + \sigma_s \right\}^6 \right], \quad (1)$$

with unit vectors $\hat{\mathbf{u}}_i, \hat{\mathbf{u}}_j$ defining the orientation of the principal axes of particles i and j , $\mathbf{r} = \mathbf{r}_j - \mathbf{r}_i \equiv r\hat{\mathbf{r}}$ the intermolecular vector of length r and σ_s and ϵ_0 are used as molecular units of length and energy. The anisotropic contact distance

$\sigma(\hat{\mathbf{u}}_i, \hat{\mathbf{u}}_j, \hat{\mathbf{r}})$ and interaction energy $\epsilon(\hat{\mathbf{u}}_i, \hat{\mathbf{u}}_j, \hat{\mathbf{r}})$ are complicated but analytical functions defined in Ref. 2. The simple GB potential allows modeling of the shape and of the nonspecific, van der Waals type, attractive interactions, in particular of the length to breadth ratio σ_e/σ_s and of the ratio of the side-by-side and end-to-end interactions ϵ_s/ϵ_e , but it does not contain specific electrostatic interactions. Here we are interested in continuing the exploration of the effects of electrostatic dipoles and we consider a potential that is the sum of a Gay–Berne (GB)^{2,3} and a dipole–dipole term:

$$U_{ij} = U_{GB} + U_{dd}. \quad (2)$$

where the dipolar contribution is given by

$$U_{dd} = \frac{\mu_i \mu_j}{r_d^3} [\hat{\boldsymbol{\mu}}_i \cdot \hat{\boldsymbol{\mu}}_j - 3(\hat{\boldsymbol{\mu}}_i \cdot \hat{\mathbf{r}}_d)(\hat{\boldsymbol{\mu}}_j \cdot \hat{\mathbf{r}}_d)], \quad (3)$$

where $\mathbf{r}_d \equiv r_d \hat{\mathbf{r}}_d$ is the vector joining the two point dipoles $\boldsymbol{\mu}_i = \mu_i \hat{\boldsymbol{\mu}}_i$, $\boldsymbol{\mu}_j = \mu_j \hat{\boldsymbol{\mu}}_j$ at distance r_d . The effect of longitudinal dipoles has been studied by various authors.^{4,5,6} The case of a transverse permanent dipole, very important in practice because of the many liquid crystals with polar lateral substituents, has been much less studied. In a first but fairly general investigation, Levesque *et al.*⁴ examined a system of 448 hard spherocylinders with aspect ratio (length L of the cylindrical part to diameter D of the capping spheres) of 5 and a strong dipole in various positions and orientations, including transverse. They found that the transverse dipole increased structuredness in the isotropic and in the smectic A. In the latter phase, interdigitation was reduced and some indications of an overall polarization were found, although a caveat was issued by the same authors about the possibility of a spurious observation. Jackson *et al.*⁸ have also studied a system of hard spherocylinders with $L/D = 5$ and a central transverse dipole. They performed NPT Monte Carlo simulations on systems with $N = 1020$ particles and found that the smectic A phase was stabilized, while the nematic disappeared altogether at low temperatures. In the smectic, and upon lowering the temperature, the very interesting observation of ring-like domains and of antiferroelectric chains of dipoles in the layer plane was made. However, it should be noticed that in the case of dipolar interactions superimposed to hard repulsive ones, the temperature dependence comes entirely from the dipolar contribution, while in a more realistic situation one might expect this to be only a fraction of the overall temperature dependence. From this point of view, the GB potential has some advantages. In the only study of which we are aware, Gwózdź *et al.*⁹ have studied a relatively small system of GB 256 particles with a central transverse dipole in a cubic box, employing the original² GB parametrization. No nematic phase was observed in this case too, while a rather surprising small tilt of the director was claimed.

Here we shall consider in detail a relatively large ($N = 1000$) GB system with a different parametrization³ and a transverse dipole in central position and we shall examine the resulting molecular organizations, paying attention to the formation of super-molecular dipolar structures.

2. The Simulations

We have performed extensive canonical ensemble (constant number of molecules N , volume V and temperature T) Monte Carlo (MC) simulations of a system of dipolar rod-like particles interacting via the potential given in Eq. (2). In particular, for the GB potential, we employ shape anisotropy $\sigma_e/\sigma_s = 3$, interaction anisotropy $\epsilon_s/\epsilon_e = 5$, cutoff $r_c^* = r_c/\sigma_s = 4.0$ and the same parametrization introduced in Ref. 3, with GB exponential coefficients $\mu = 1$, $\nu = 3$, that has the advantage of offering a wider nematic range compared to the standard choice of $\mu = 2$, $\nu = 1$.² Molecular orientation is defined with respect to the principal axes of particles i and j , namely $\hat{\mathbf{u}}_i \equiv \hat{\mathbf{z}}_i$ and $\hat{\mathbf{u}}_j \equiv \hat{\mathbf{z}}_j$. In this framework, we consider transverse dipole moments $\boldsymbol{\mu}_i^* \equiv \mu^* \hat{\mathbf{x}}_i$, $\boldsymbol{\mu}_j^* \equiv \mu^* \hat{\mathbf{x}}_j$ (we use the dimensionless $\mu^* \equiv \mu/(\epsilon_0 \sigma_s^3)^{1/2}$ and $r_d^* \equiv r_d/\sigma_s$) positioned in the center of the molecule. We use a dimensionless dipole moment $\mu^* = 2$ that, assuming a molecular cross section $\sigma_s = 5 \text{ \AA}$ and an energy scale $\epsilon_0/k = 100 \text{ K}$, would correspond to about 2.6 D. Our sample consists of $N = 1000$ interacting particles enclosed in a cubic box with periodic boundary conditions at a dimensionless density $\rho^* \equiv N\sigma_s^3/V = 0.3$ and for several temperatures $T^* \equiv kT/\epsilon_0$ in the range 4.0–1.6.

The dipolar energy for particles in the box surrounded by its periodic images has been computed using both the very reliable but time consuming Ewald sum technique¹⁰ with tin foil boundary conditions, and the more approximate Reaction Field¹¹ method, with cutoff $r_{RF}^* = 6.0$ and dielectric constant of the surrounding medium $\epsilon_{RF} = 1.5$. We have found that, for our model and sample size, the two methods give essentially the same results for the energy (within 0.01%) as recently found for other dipolar systems.^{12,13} We also find the use of tin foil boundary conditions ($\epsilon_{RF} = \infty$) for the Reaction Field to be satisfactory, in agreement with Ref. 13. Thus, as the Reaction Field method is an order of magnitude faster for our sample size, we have used this approach for the large majority of calculations and

Table 1. Results from the Monte Carlo simulation of $N = 1000$ systems of GB rod-like molecules with central transverse dipole $\boldsymbol{\mu}_i^* = \mu^* \hat{\boldsymbol{\mu}}_i$, with $\hat{\boldsymbol{\mu}}_i \equiv \hat{\mathbf{x}}_i$ and $\mu^* = 2$ at several dimensionless temperatures T^* corresponding to the phases indicated. We report the number of equilibration n_{eq} and production n_{prod} cycles (1 cycle = N moves), the energy $\langle U^* \rangle$, the order parameter $\langle P_2 \rangle = \langle R_{0,0}^2 \rangle = \langle (3 \cos^2 \beta - 1)/2 \rangle$ and the biaxial order parameter $\langle R_{2,2}^2 \rangle = \langle (1 + \cos^2 \beta) \cos(2\alpha) \cos(2\gamma)/4 \rangle$, where α, β, γ are the Euler angles between molecular axes and director.

T^*	$n_{eq}/10^3$	$n_{prod}/10^3$	Ph	$\langle U^* \rangle$	$\langle P_2 \rangle$	$\langle R_{2,2}^2 \rangle$
1.6	200	150	S_B	-18.7 ± 0.1	0.97 ± 0.02	0.02 ± 0.01
2.0	200	150	S_B	-17.3 ± 0.2	0.96 ± 0.02	0.02 ± 0.01
2.4	200	150	S_B	-15.9 ± 0.2	0.94 ± 0.02	0.01 ± 0.01
2.8	200	150	S_A	-14.0 ± 0.2	0.92 ± 0.02	0.01 ± 0.01
3.4	500	300	N	-7.3 ± 0.2	0.67 ± 0.02	0.01 ± 0.01
4.0	200	150	I	-4.0 ± 0.2	0.10 ± 0.02	0.01 ± 0.01

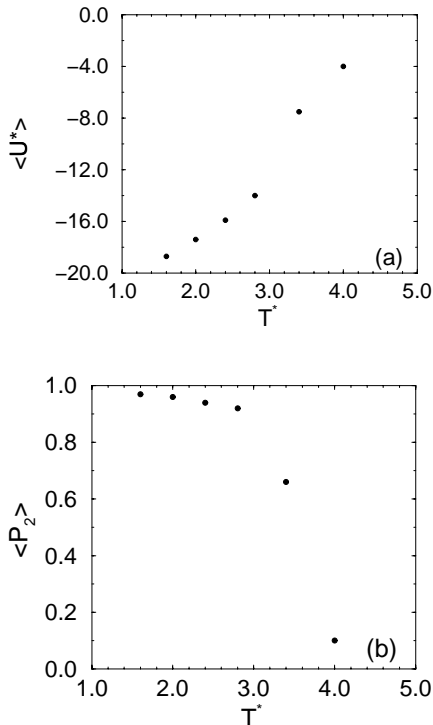


Fig. 1. Average energy $\langle U^* \rangle$ (1(a)) and average orientational order parameter $\langle P_2 \rangle$ (1(b)) plotted against the dimensionless temperature T^* for the system of particles with central transverse dipoles.

the Ewald technique mainly to check the results.

The runs were started from dipole-less equilibrium configurations and equilibrated with transverse dipolar interactions switched on for over 200 000 cycles with production runs of 150–200 000 cycles. We report in Table 1 the main results for the energy $\langle U^* \rangle = \langle U \rangle / \epsilon_0$ and the molecular \hat{z}_i axis order parameter $\langle P_2 \rangle = \langle R_{0,0}^2 \rangle$ and the biaxial order parameter $\langle R_{2,2}^2 \rangle$ (defined and computed as in Ref. 14) for the different phases observed: isotropic (I), nematic (N), smectic A (S_A) and smectic B (S_B). The order parameter $\langle P_2 \rangle$, plotted in Fig. 1(b), shows the familiar decrease with increasing temperature. The rod with a transverse dipole is a biaxial particle and we investigated the existence of long-range biaxial order. We find that in all the cases studied, the biaxial order parameter $\langle R_{2,2}^2 \rangle$ is essentially zero (as shown in Table 1). We shall now consider the simulation results in some detail.

3. Results

The system presents an isotropic, nematic and smectic phase as shown by the radial distribution $g_0(r) = \langle \delta(r - r_{ij}) \rangle_{ij} / (4\pi r^2 \rho)$ (see Fig. 2) and by the density along the director $g(z) = \langle \delta(z - z_{ij}) \rangle_{ij} / (\pi R^2 \rho)$ (see Fig. 3), where $z_{ij} = r_{ij} \cos \beta_{r_{ij}}$ is

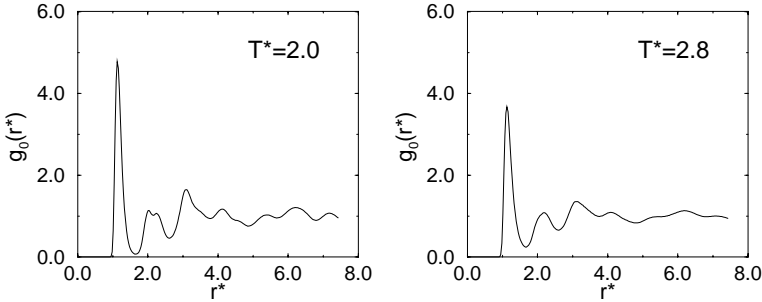


Fig. 2. Radial distribution $g_0(r^*)$ for the system of rods with central transverse dipoles at the temperatures $T^* = 2.0$ (S_B) and 2.8 (S_A).

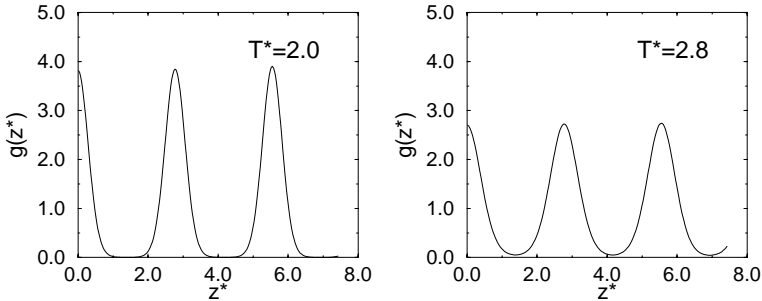


Fig. 3. Density along the director $g(z^*)$ for the system of rods with central transverse dipoles at the temperatures $T^* = 2.0$ (S_B) and 2.8 (S_A).

measured with respect to the director frame and R is the radius of the cylindrical sampling region.

The radial distribution in particular shows a sharp peak at $r^* = 1$, corresponding to the preferred side-by-side nearest-neighbor configuration. At the lowest temperatures ($T^* = 1.6$ and 2.0) the radial distribution shows also a splitting of the second peak characteristic of a hexagonal order in the plane and thus of a smectic B-type ordering, at least over the distances amenable to our sample size (cf. Ref. 3).

The density profile across the sample (Fig. 3) shows a clear smectic periodicity at $T^* = 2.0$ and 2.8 . The peaks are essentially centered at multiples of the molecular length σ_e , showing that very little interdigitation of the layers exists in this case.

The correlation between molecular axes can be represented, in general, by averages of rotational functions $S_{m_1, m_2}^{L_1, L_2, L_3}$ ¹⁵ as a function of separation r . In Fig. 4, we show the orientational correlation function

$$\begin{aligned} \text{Re}[S_{2,2}^{2,2,0}(r)] = \frac{1}{4\sqrt{5}} \langle \delta(r_{ij} - r) [(\hat{\mathbf{x}}_i \cdot \hat{\mathbf{x}}_j)^2 - (\hat{\mathbf{x}}_i \cdot \hat{\mathbf{y}}_j)^2 - (\hat{\mathbf{y}}_i \cdot \hat{\mathbf{x}}_j)^2 \\ + (\hat{\mathbf{y}}_i \cdot \hat{\mathbf{y}}_j)^2 - 2(\hat{\mathbf{x}}_i \cdot \hat{\mathbf{y}}_j)(\hat{\mathbf{y}}_i \cdot \hat{\mathbf{x}}_j) - 2(\hat{\mathbf{x}}_i \cdot \hat{\mathbf{x}}_j)(\hat{\mathbf{y}}_i \cdot \hat{\mathbf{y}}_j)] \rangle_{ij}. \quad (4) \end{aligned}$$

The limiting value for $r \rightarrow \infty$ of this correlation is the combination of biaxial order parameters $[\langle R_{0,2}^2 \rangle^2 + 2\langle R_{2,2}^2 \rangle^2]\sqrt{5}$, where $\langle R_{0,2}^2 \rangle$ is also defined in Ref. 14. We see

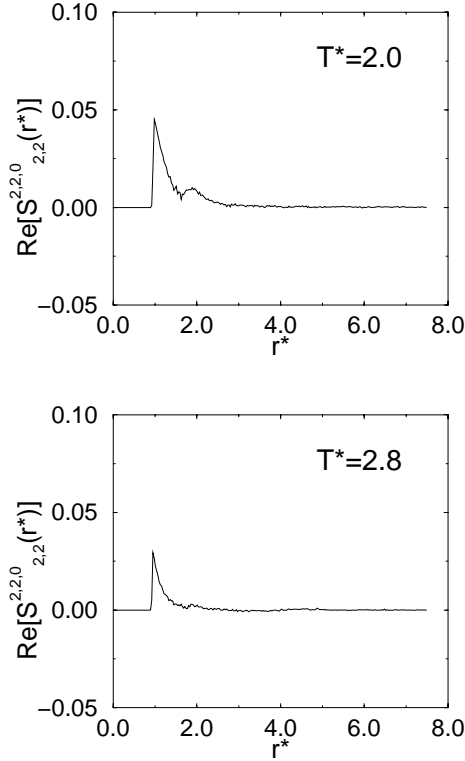


Fig. 4. Orientational correlation function $\text{Re}[S_{2,2}^{2,2,0}(r^*)]$ for the system of rods with central transverse dipoles at the temperatures $T^* = 2.0$ (S_B) and 2.8 (S_A).

that, apart from the positional order and the long-range orientational order (see Table 1), the system does not give rise to a biaxial structure; in other words the short axes of the molecules are only ordered at short, but not at long range, as we have already mentioned before.

In order to investigate the correlation functions between molecular dipoles, we calculate

$$S_{1,\pm 1}^{1,1,0}(r) = \frac{1}{2\sqrt{3}} \langle \delta(r_{ij} - r) [\mp \hat{\mathbf{x}}_i \cdot \hat{\mathbf{x}}_j + \hat{\mathbf{y}}_i \cdot \hat{\mathbf{y}}_j + i(\hat{\mathbf{x}}_i \cdot \hat{\mathbf{y}}_j \pm \hat{\mathbf{y}}_i \cdot \hat{\mathbf{x}}_j)] \rangle_{ij}. \quad (5)$$

In practice, we find it more convenient here to plot a linear combination of these invariants, giving the average scalar product between the transverse components of the dipole of a molecule i chosen as the origin and that of any molecule j found at a distance r , that is

$$\langle \delta(r_{ij} - r) [\hat{\mathbf{x}}_i \cdot \hat{\mathbf{x}}_j] \rangle_{ij} = -\sqrt{3} \text{Re}[S_{1,1}^{1,1,0}(r) - S_{1,-1}^{1,1,0}(r)]. \quad (6)$$

At the lowest temperatures, the molecules are, as we have seen, well ordered in layers and the dipoles are essentially distributed in the layer planes. In Fig. 5 we see that in the smectic phases, the dipoles within the first two nearest-neighbor

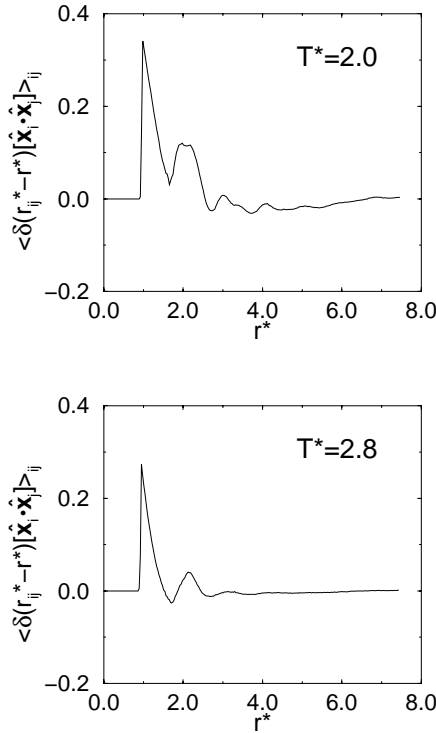


Fig. 5. Dipolar pair correlation function $\langle \delta(r_{ij}^* - r^*) [\hat{\mathbf{x}}_i \cdot \hat{\mathbf{x}}_j] \rangle_{ij}$ for the system of rods with central transverse dipoles at dimensionless temperatures $T^* = 2.0$ (S_B), and 2.8 (S_A).

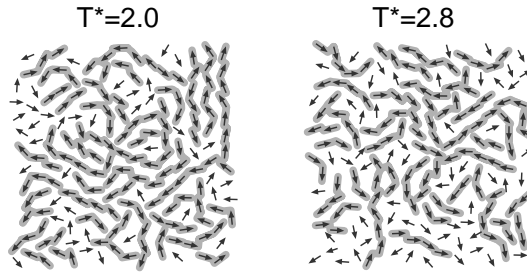


Fig. 6. The dipolar organization in a smectic layer for the central transverse dipole system at $T^* = 2.0$ (S_B) and $T^* = 2.8$ (S_A). Chains of dipoles are visualized using a gray shading. Two dipoles $\boldsymbol{\mu}_i, \boldsymbol{\mu}_j$ lying on the same smectic layer are considered “chained” whenever $\hat{\boldsymbol{\mu}}_i \cdot \hat{\boldsymbol{\mu}}_j \geq 0.3$ and $r_d^* \leq 1.5$.

coordination shells are, on average, parallel. A snapshot of dipole configurations, presented in Fig. 6, is rather illuminating in this respect and shows chains and rings of dipoles, visualized here with a gray shading as a guide to the eye, as already discovered by Jackson *et al.*⁸ for their dipolar spherocylinders. These structures were not reported by Gwózdź *et al.*,⁹ possibly due to the limited size of their

system. In any case, the dipolar chains do not seem to be just a feature of the hard spherocylinders model in Ref. 8, but are present also in the attractive-repulsive Gay–Berne systems.

4. Discussion and Conclusions

We have simulated in detail a system of rod-like Gay–Berne particles containing a permanent point dipole perpendicular to the long axis and located in the center of the molecule. The system shows enhanced layering with little interdigitation and formation of chains and rings of dipoles in the layer plane.

Acknowledgments

We thank the University of Bologna, MURST, CNR and EU (TMR-FMRX CT9701121) for support.

References

1. S. Chandrasekhar, *Liquid Crystals*, 2nd edition (Cambridge University Press, Cambridge, 1992).
2. J. G. Gay and B. J. Berne, *J. Chem. Phys.* **74**, 3316 (1981).
3. R. Berardi, A. P. J. Emerson, and C. Zannoni, *J. Chem. Soc. Faraday Trans.* **89**, 4069 (1993).
4. D. Levesque, J. J. Weis, and G. J. Zarragoicoechea, *Phys. Rev. E* **47**, 496 (1993).
5. J. J. Weis, D. Levesque, and G. J. Zarragoicoechea, *Mol. Phys.* **75**, 989 (1992); *ibid*, *Mol. Phys.* **80**, 1077 (1993).
6. R. Berardi, S. Orlandi, and C. Zannoni, *Chem. Phys. Lett.* **261**, 363 (1996).
7. K. Satoh, S. Mila, and S. Kondo, *Liq. Cryst.* **20**, 757 (1996); *ibid*, *Chem. Phys. Lett.* **255**, 99 (1996).
8. A. Gil-Vilegas, S. McGrother, and G. Jackson, *Chem. Phys. Lett.* **269**, 441 (1997).
9. E. Gwózdź, A. Bródka, and K. Pasterny, *Chem. Phys. Lett.* **267**, 557 (1997).
10. S. W. De Leeuw, J. W. Perram, and E. R. Smith, *Proc. R. Soc. Lond. A* **373**, 57 (1980).
11. J. A. Barker and R. O. Watts, *Mol. Phys.* **26**, 789 (1973).
12. A. Gil-Vilegas, S. McGrother, and G. Jackson, *Mol. Phys.* **92**, 723 (1997).
13. M. Houssa, A. Oualid, and L. F. Rull, *Mol. Phys.* **94**, 439 (1998).
14. F. Biscarini, C. Chiccoli, P. Pasini, F. Semeria, and C. Zannoni, *Phys. Rev. Lett.* **75**, 1803 (1995).
15. A. J. Stone, *Mol. Phys.* **36**, 241 (1978).